CENTRAL RESEARCH LIBRARY
DOCUMENT COLLECTION

OAK RIDGE NATIONAL LABORATORY
OPERATED BY
UNION CARBIDE CORPORATION
NUCLEAR DIVISION

POST OFFICE BOX X
OAK RIDGE, TENNESSEE 37830

ORNL-MIT- 84

DATE: June 4, 1969

COPY NO. 28

SUBJECT: A Study of the Dispersion of Gases in Viscous Liquids with Application to Radioactive Krypton and Xenon Disposal, Part II

AUTHOR: W.A. Heath and M.H. Jorris

Consultants: W.E. Clark and W.F. Schaffer, Jr.

ABSTRACT

The dispersion of argon in polybutene was further investigated by studying the effects of input power, impeller blade pitch, and liquid flow rate on the loading achievable. A gas dispersion model relating gas loading to input power and liquid flow rate was proposed based on the experimental results. This model correlated the experimental data in a form

$$\ln\left[\frac{\phi_{max} - \phi}{\phi_{max}}\right] = \frac{kP}{L}$$

where ϕ is the volumetric gas loading, P is the input power, L is the liquid flow rate, and k is a constant.

OAK RIDGE NATIONAL LABORATORY
CENTRAL RESEARCH LIBRARY
DOCUMENT COLLECTION
LIBRARY LOAN COPY
DO NOT TRANSFER TO ANOTHER PERSON
If you wish someone else to see this document, send in name with document and the library will arrange a loan.

Oak Ridge Station
School of Chemical Engineering Practice
Massachusetts Institute of Technology

[redacted]

CONTENTS

Page

1. Summary 4
2. Introduction 4
   2.1 Background 4
   2.2 Previous Work 5
   2.3 Present Study 5
3. Experimental Apparatus and Procedure 5
4. Results 8
   4.1 Scoping Experiments 8
   4.2 Effect of Impeller Pitch on Percent Loading at Constant Power Input 8
   4.3 Effect of Impeller Speed and Power Input on Percent Loading 10
5. Discussion of Results 10
   5.1 Description of Proposed Mixing Model 10
   5.2 Gas Loading Experiments 15
6. Conclusions 15
7. Recommendations 17
8. Acknowledgement 17
9. Appendix 18
   9.1 Physical Properties of Polybutene 16 18
   9.2 Experimental Data 18
   9.3 Viscosity Measurements 19
   9.4 Location of Original Data 21
   9.5 Nomenclature 21
   9.6 Bibliography 22

1. SUMMARY

This study was conducted to further investigate parameters affecting the dispersion of argon in polybutene. (Argon and polybutene were chosen as model fluids to simulate the dispersion of radioactive krypton and xenon in molten glass.) The experimental apparatus used was a cylindrical lucite chamber equipped with a variable speed impeller, gas and polybutene inlets, foam withdrawal ports, and pressure and temperature measurement capability. The effects of input power, impeller blade pitch and liquid flow rate on gas loading and viscosity were studied. It was found that at a constant input power to the impeller motor of 155 w, impeller blade pitch had no significant effect on gas loading. An increase in input power was found to increase gas loading, but indications were that maximum gas loading at zero liquid flow rate was independent of input power. The maximum gas loading obtained was 23% at 6900 rpm with a liquid flow rate of 165 ml/min and input power of approximately 190 w. A model based on bubble formation rate as a function of power input and gas loading was postulated to characterize the dispersion mechanism.

The viscosity of the foam at various gas loadings was measured. It was found that up to 23% gas loading, the foam exhibits Newtonian characteristics and that the foam viscosity was greater than that of pure polybutene at the same temperature. No trend was observed between the foam viscosity and the percent gas loading. Fluid temperature had a large effect on viscosity, but the effect was not investigated fully.

It is recommended that future work be done to substantiate and further develop the proposed model of the dispersion mechanism, and to determine the effect of viscosity on foam formation. Such studies would provide guidelines for extrapolating experimental results obtained with the polybutene model fluid to molten glasses with somewhat different fluid properties.

2. INTRODUCTION

2.1 Background

Methods for disposing of radioactive waste gases from nuclear fuel reprocessing plants are currently being evaluated at Oak Ridge National Laboratory. The radioactive isotopes of krypton and xenon are of particular interest since they cannot be converted to solid compounds for simple storage. One of the proposed methods of disposal is containment of krypton and xenon as small bubbles in a glass matrix. The thermal and mechanical properties of such a glass foam are desirable for long term storage of the radioactive waste gases. In addition, glass foams would be relatively safe in the event of accidental breakage since only a small fraction of the radioactive gas would escape.

2.2 Previous Work

An earlier Practice School group (3) performed a preliminary study of the dispersion of gases in highly viscous liquids. Experiments were conducted to determine the effect of operating variables such as gas flow rate, impeller speed, impeller geometry, and mixing time, on the bubble size and size distribution, and on the volumetric percent gas loading. As a result of the earlier work, a new mixing chamber intended to enhance mixing in the vicinity of the impeller and to eliminate bypassing of the viscous fluid around the impeller was constructed for use in the present study. Relevant literature references to previous work are included in Appendix 9.6.

2.3 Present Work

The objective of this study was to experimentally determine the important parameters affecting the foaming of highly viscous liquids. The study differs from most previous mixing work in three respects: (1) a large impeller to tank diameter was employed, (2) a highly viscous liquid was used to form the gas-liquid foam, and (3) an unbaffled mixing chamber was used.

To provide data for scaleup to a molten glass system, we investigated the effects on foam formation of power input, liquid flow rate, and impeller geometry. A simplified mechanistic model for the formation of bubbles based on power input and volume percent of gas in the foam was developed and used to correlate the data from this study.

3. EXPERIMENTAL APPARATUS AND PROCEDURE

To simulate the formation of foams of radioactive krypton and xenon in molten glass, argon and polybutene grade 16 (see Appendix 9.1) were used as model fluids in this experiment. The apparatus used to produce the foam consisted of a 55-gal polybutene feed drum, a lucite mixing chamber (3 in. I.D. x 8 in. high), a receiving tank for the foam discharged from the mixing chamber, and a recirculating pump (see Fig. 1).

The polybutene feed drum was mounted approximately 2 ft above the mixing chamber, and a ball valve was available on the outlet line from the drum to allow control of the liquid flow rate. It was possible to pressurize the feed drum to 6.5 psig to obtain a maximum polybutene flow rate of 550-600 ml/min. The residence time in the drum was sufficient for the recirculated foam to release its bubbles before being fed to the mixing chamber.

The mixing chamber (Fig. 2A) was a lucite cylinder with a removable top and multiple gas inlet and foam exit ports. Argon was introduced into

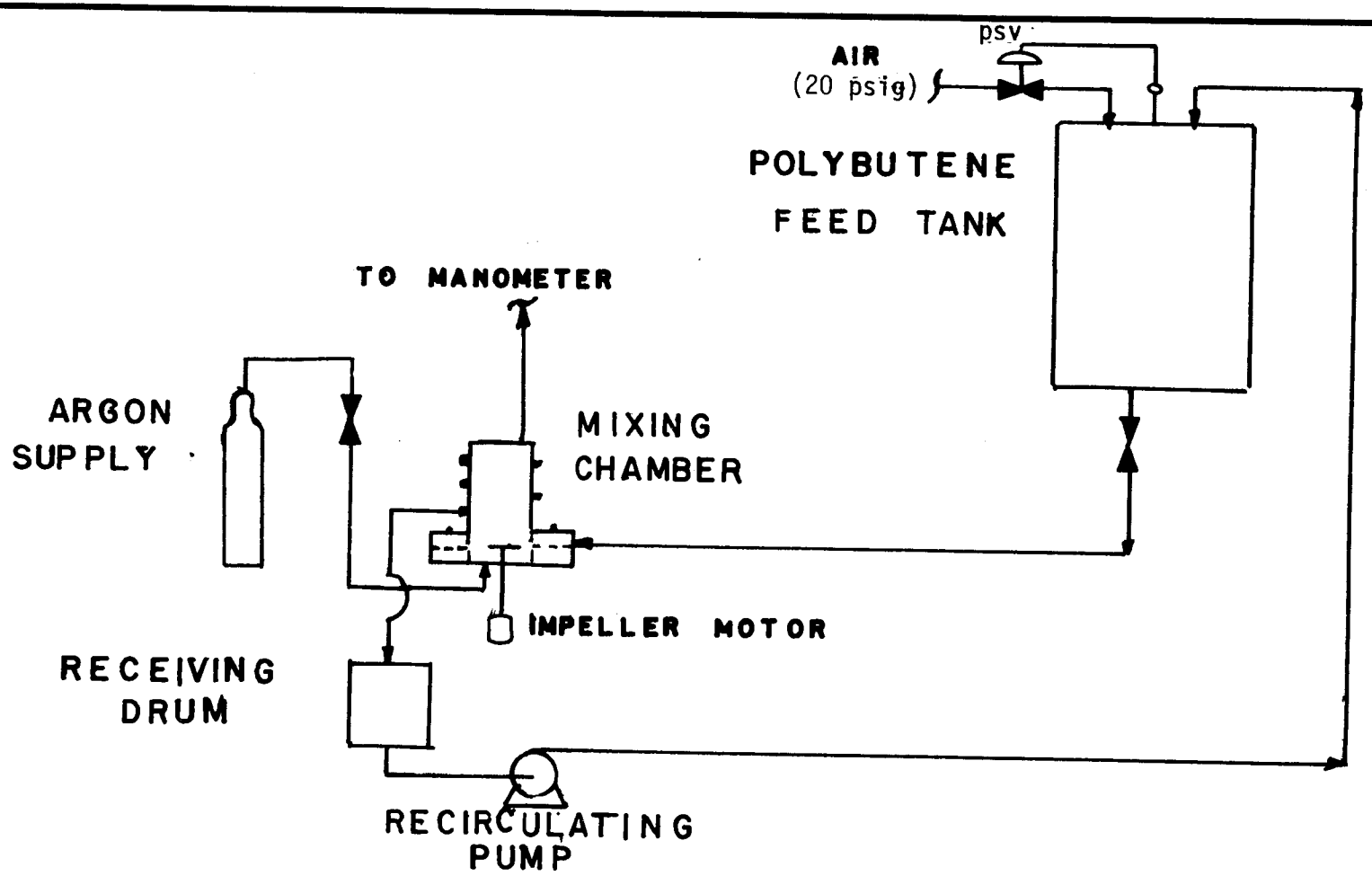

MASSACHUSETTS INSTITUTE OF TECHNOLOGY
SCHOOL OF CHEMICAL ENGINEERING PRACTICE
AT
OAK RIDGE NATIONAL LABORATORY

SCHEMATIC DIAGRAM OF APPARATUS

DATE	DRAWN BY	FILE NO.	FIG.
6-3-69	WAH	CEPS-X-84	1

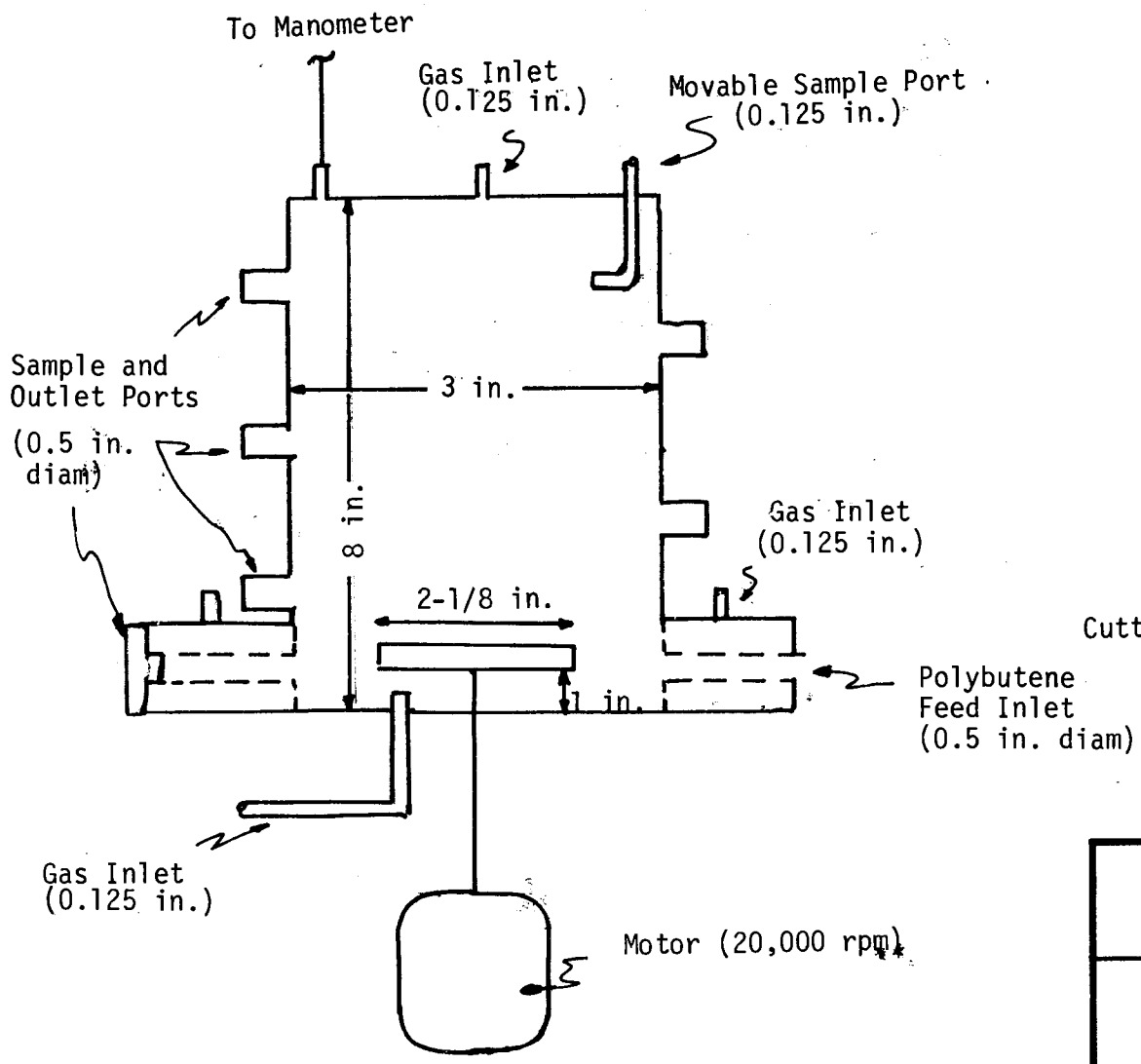

A. MIXING CHAMBER

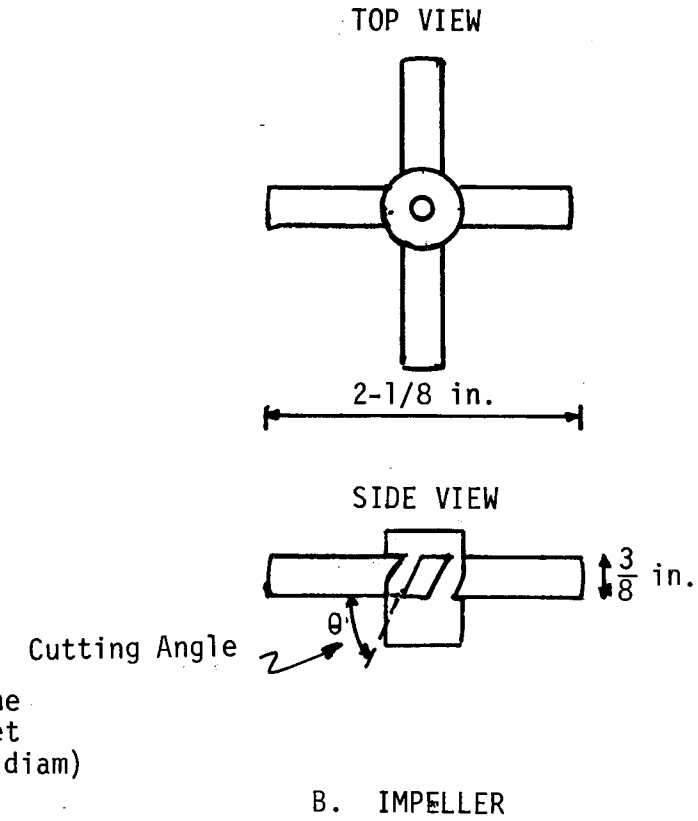

B. IMPELLER

MASSACHUSETTS INSTITUTE OF TECHNOLOGY
SCHOOL OF CHEMICAL ENGINEERING PRACTICE
AT
OAK RIDGE NATIONAL LABORATORY

DIAGRAM OF MIXING
CHAMBER AND IMPELLER

DATE	DRAWN BY	FILE NO.	FIG.
6-3-69	WAH	CEPS-X-84	2

the chamber through an 1/8 in. copper tube connected to a pressurized cylinder of argon.

The five impellers studied for foaming the liquid-gas mixture were 2-1/8 in. diameter with 0°, 15°, 30°, 45°, and 90° pitches (Fig. 2B). The impellers (located 1-1/16 in. above the bottom of the mixing chamber) were driven by a 20,000 rpm motor located below the chamber. All experiments in the mixing chamber were conducted with a liquid vortex above the impeller.

Foam samples for determination of percent loading were obtained by running the outlet stream into a graduated cylinder until 90-100 ml of foam had been collected. Foam removal from the chamber was accomplished by overflow through an outlet port. The gas pressure above the foam was always greater than atmospheric pressure.

Viscosity data were obtained using a Brookfield viscometer.

4. RESULTS

4.1 Scoping Experiments

Two groups of preliminary experiments were conducted to obtain some basic operating information about the apparatus. In the first group four different gas injection locations were compared: (1) gas through the top of the chamber, (2) gas fed into the inlet stream, (3) gas injected into the fluid through the side of the chamber opposite the polybutene feed stream, and (4) gas injected through the chamber bottom beneath the impeller. The loadings obtained in the first three cases were 5.4% whereas the loading obtained in the fourth case was 6.6%. Because greater loading was obtained by feeding the gas beneath the impeller, this feed position was used in all succeeding experiments.

The second set of experiments conducted was concerned with the homogeneity of the foam in the mixing chamber. Foam samples withdrawn from the side of the mixing chamber and from the top of the vortex has volumetric loadings of 22.2% and 18.1%, respectively. The 10% variation was not considered significant, so the mixing chamber was considered to be a well-mixed tank.

Viscosity measurements were made on foams at different loadings. Results indicating the foams under 23% volumetric loading are Newtonian at short times are given in Appendix 9.3.

4.2 The Effect of Impeller Pitch on Percent Loading at Constant Power Input

Figure 3 shows that the percent loading is about 15% and is independent of the impeller pitch at a constant power input to the motor of 155 w (uncorrected for motor losses) and a liquid flow rate of 73 ml/min. Geometrically similar vortices were maintained over each impeller by adjusting the liquid height in the mixing chamber. This required that the volume of foam in the chamber increased as the impeller pitch was varied from 0°

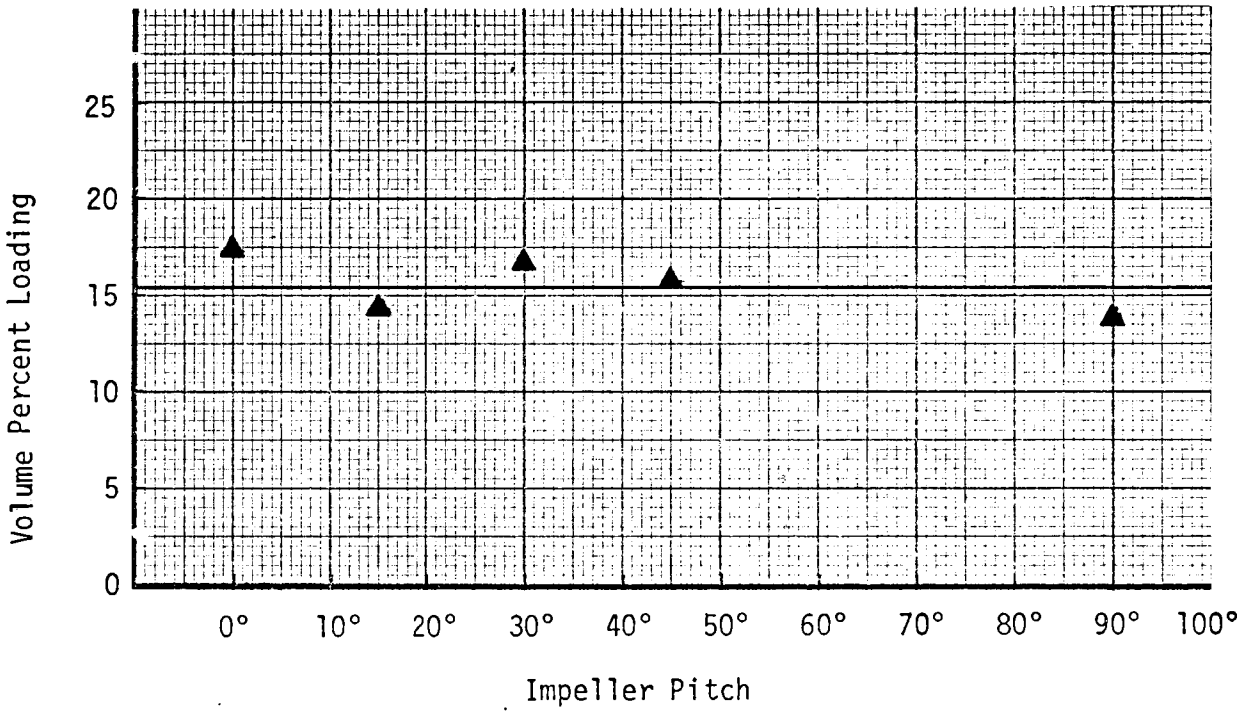

Power Input = 155 watts
Liquid Flow Rate = 74 ml/min

MASSACHUSETTS INSTITUTE OF TECHNOLOGY
SCHOOL OF CHEMICAL ENGINEERING PRACTICE
AT
OAK RIDGE NATIONAL LABORATORY

Effect of Impeller Pitch on
Gas Loading at Constant Power

DATE	DRAWN BY	FILE NO.	FIG.
6-3-69	WAH	CEPS-X-84	3

to 90°. The increase in volume was about 33%, and, therefore, liquid residence time was not constant. The liquid height in the mixing chamber was varied by controlling the argon pressure above the vortex. The gas pressures varied from 0.26 to 0.28 psig.

4.3 The Effect of Impeller Speed and Power Input on Percent Loading

Figure 4 shows the effect of power input (uncorrected for motor losses) on percent loading. The maximum loading obtained was 22.4% at a power input of 189 w and a liquid flow rate of 166 ml/min. Because of problems encountered with the impeller bearing, data at higher power inputs could not be obtained. The same problem allowed only one experimental point to be taken at flow rates of 73 and 95 ml/min. The height of the foam in the mixing chamber was held constant at 3-1/4 in. above the bottom for all liquid flow rates.

Table 3 in Appendix 9.2 contains the data used to construct Fig. 4. Experimental Runs A, B, C, D, and J were considered to be 170 ml/min, the average flow rate for the five runs. The variations in the measured liquid flow rate may have resulted from experimental error. Due to binding of the impeller bearing, the results from Run B were not plotted in Fig. 4. Runs E, F, G, and H were taken to be at a flow rate of 550 ml/min, the approximate average of Runs E, G, and H. The high liquid rate obtained for Run F appears in error since the liquid head and chamber gas pressures were no greater than for other runs in which the liquid rates were 500 and 650 ml/min. Because of the very short time (and corresponding large error) required to collect the 100 ml of foam in measuring the flow rate, the liquid rates are probably the same within experimental error. A larger sample collection vessel should have been used to decrease the error associated with liquid flow rate measurements.

Table 3 (Appendix 9.2) also shows that a greater power input was required to produce the same impeller speed at a larger liquid flow rate.

5. DISCUSSION OF RESULTS

5.1 Description of Proposed Mixing Model

The results indicated that one could describe the rate of bubble formation as

$$\frac{dN^+}{d\theta} = k_1 P \qquad (1)$$

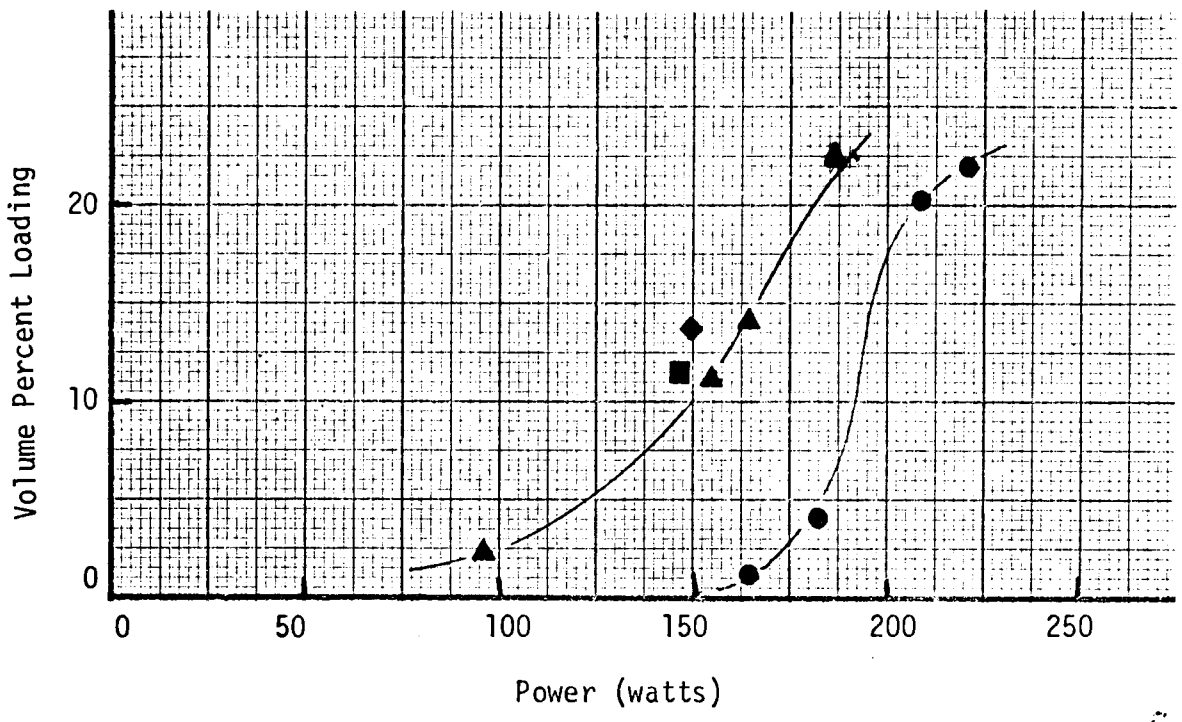

◆ L = 73 ml/min
■ L = 95 ml/min
▲ L = 170 ml/min
● L = 550 ml/min

MASSACHUSETTS INSTITUTE OF TECHNOLOGY
SCHOOL OF CHEMICAL ENGINEERING PRACTICE
AT
OAK RIDGE NATIONAL LABORATORY

PERCENT LOADING AS A FUNCTION OF POWER INPUT AND LIQUID FLOW RATES

DATE	DRAWN BY	FILE NO.	FIG.
6-3-69	WAH	CEPS-X-84	4

where N^+ is the number of bubbles formed, θ is time, P is power input, and k_1 is a rate constant. Equation (1) is plausible since the experimental loadings (and consequently N) increased with the power input at a given liquid flow rate.

One can also postulate that the rate of bubble destruction or loss is given by,

$$\frac{dN^-}{d\theta} = k_2 P \phi \tag{2}$$

where N^- is the number of bubbles destroyed or lost and ϕ is the volumetric gas loading. One would expect that as the power increased, the rate at which new liquid foam was brought to the vortex surface would increase, thus allowing the bubbles a greater chance of escape. In addition, as loading increases, there is a greater probability of bubble loss by their breaking through the surface of the fluid.

Combining Eqs. (1) and (2), one obtains for the net rate of bubble formation,

$$\frac{dN}{d\theta} = k_1 P - k_2 P \phi \tag{3}$$

By defining the loading as,

$$\phi = \frac{Nv}{V} \tag{4}$$

where v is the bubble volume (assumed constant at a single power), and V is the foam volume in the mixing chamber, Eq. (3) becomes,

$$\frac{dN}{d\theta} = k_1 P - k_2 P \frac{Nv}{V} \tag{5}$$

Integrating Eq. (5) with the boundary conditions

$$N = 0 \text{ at } \theta = 0$$

$$N = N \text{ at } \theta = \tau$$

where τ is the chamber residence time one obtains,

$$\ln\left(1 - \frac{k_2}{k_1}\phi\right) = -k_2 \frac{P \tau v}{V} \tag{6}$$

For low loadings, one may approximate the residence time as

$$\tau = \frac{V(1 - \phi)}{L} \simeq \frac{V}{L} \tag{7}$$

Substituting into Eq. (6) yields,

$$\ln\left(1 - \frac{k_2}{k_1}\phi\right) = -k_2\left(\frac{Pv}{L}\right) \tag{8}$$

When the liquid flow rate is set at zero, the loading obtained should be the maximum possible. Then,

$$\phi_{max} = \frac{k_1}{k_2}$$

and Eq. (8) becomes,

$$\ln(\phi_{max} - \phi) = \ln \phi_{max} - \frac{Pk_2v}{L} \tag{9}$$

Equation (9) shows that if $\ln(\phi_{max} - \phi)$ is plotted against $1/L$, the curves should be straight lines with slopes equal to $-Pk_2v$ and a common intercept equal to $\ln \phi_{max}$. Figure 5 shows that the experimental data follow the predicted model quite well. The maximum loading (ϕ_{max}) was taken as 24.8%, the value which Jorris and Bowers (3) obtained in their experimental work using a Waring blender to produce the gas-liquid foam. Since ϕ_{max} is only a function of k_1 and k_2, one would expect all loadings to approach the same maximum loading independent of the power input.

There are four features of this model to be discussed.

1. The assumption that ϕ is small compared to 1.0 [see Eq. (7)] is not valid at low liquid flow rates where ϕ is greater than 0.1. It is therefore expected that the curves in Fig. 5 should be less steep as the value of $(\phi_{max} - \phi)$ decreases. This is not shown in Fig. 5 because of the limited accuracy of the data.

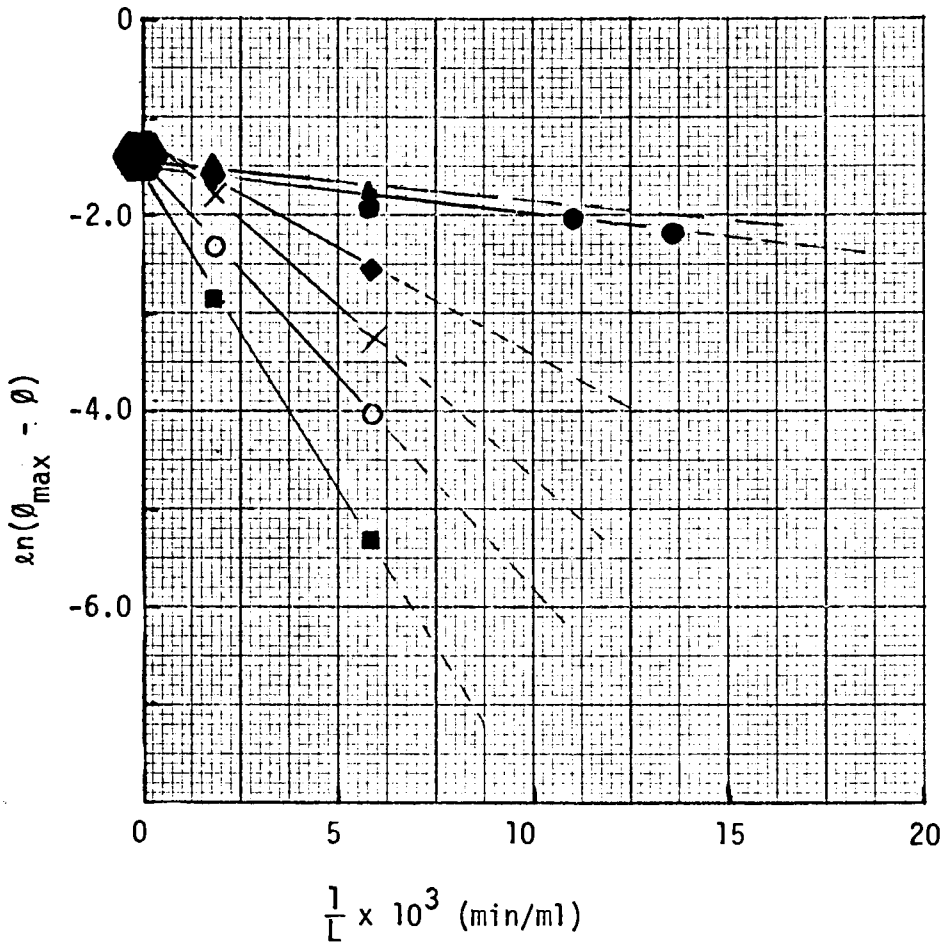

▲ - 75 watts
● - 150 watts
◆ - 175 watts
× - 185 watts
○ - 195 watts
■ - 205 watts
⬢ - $Ø_{max}$

MASSACHUSETTS INSTITUTE OF TECHNOLOGY
SCHOOL OF CHEMICAL ENGINEERING PRACTICE
AT
OAK RIDGE NATIONAL LABORATORY

$\ell n(Ø_{max} - Ø)$ As a Function of the Liquid Flow Rate

DATE	DRAWN BY	FILE NO.	FIG.
6-3-69	WAH	CEPS-X-84	5

2. The model predicts that k_2v will decrease with increasing power. This decrease is shown in Fig. 6, a plot of k_2v as a function of power. (The term k_2v was obtained from the slopes of the power curves in Fig. 5). The decrease in k_2v with power probably results from a decrease in v, since k_1/k_2 (i.e., $\emptyset_{max}$) is independent of power, and it is improbably that this ratio would remain constant if k_2 were a function of power. A decreasing bubble volume does not contradict any assumptions made in the model since the model required only that bubble volume be the same for all bubbles at a given power. One might physically expect that the bubble volume would decrease with increasing power.

3. Equation (9) indicates that the loading is independent of the volume of foam in the mixing chamber. In all experiments conducted, the foam volume in the mixing chamber was held approximately constant. Variations in this volume should be considered in future work since at this time no distinction can be made between $\emptyset$ and N dependence.

4. The effect of viscosity (and consequently its determining variables temperature fluid type and loading) has not been accounted for mechanistically. Since this parameter was not controlled in our experiments, its effect may be included in other variables in Eq. (9) (e.g., power). The present model should be extended to include data on more viscous grades of polybutene, which are closer to the conditions of molten glass. This might be done by using blender experiments to obtain $\emptyset_{max}$ for higher viscosity fluids and determining the constant k_2v as a function of power input for the more viscous fluids (as discussed in point 2 above).

5.2 Gas Loading Experiments

Loading as a function of impeller pitch was determined at constant power input with impeller speeds varying from 3440 rpm for the zero degree impeller to 2540 rpm for the 90° impeller. Within the accuracy of the data, no effect of impeller pitch on loading was observed. This is consistent with the proposed mixing model which indicates that at constant power input, constant liquid flow rate, and constant bubble size, one would obtain a single gas loading. Visual observation of the foam under a microscope indicated that the bubble diameter was the same for each of the impellers.

6. CONCLUSIONS

1. It is possible to obtain gas loadings (in liquids of viscosity approximately 20 poise) of at least 23% in a flow system at impeller speeds of 5000-7000 rpm.

2. It is possible to describe the mixing mechanism by a model which postulates that the rate of bubble formation is a function of the power input and percent loading.

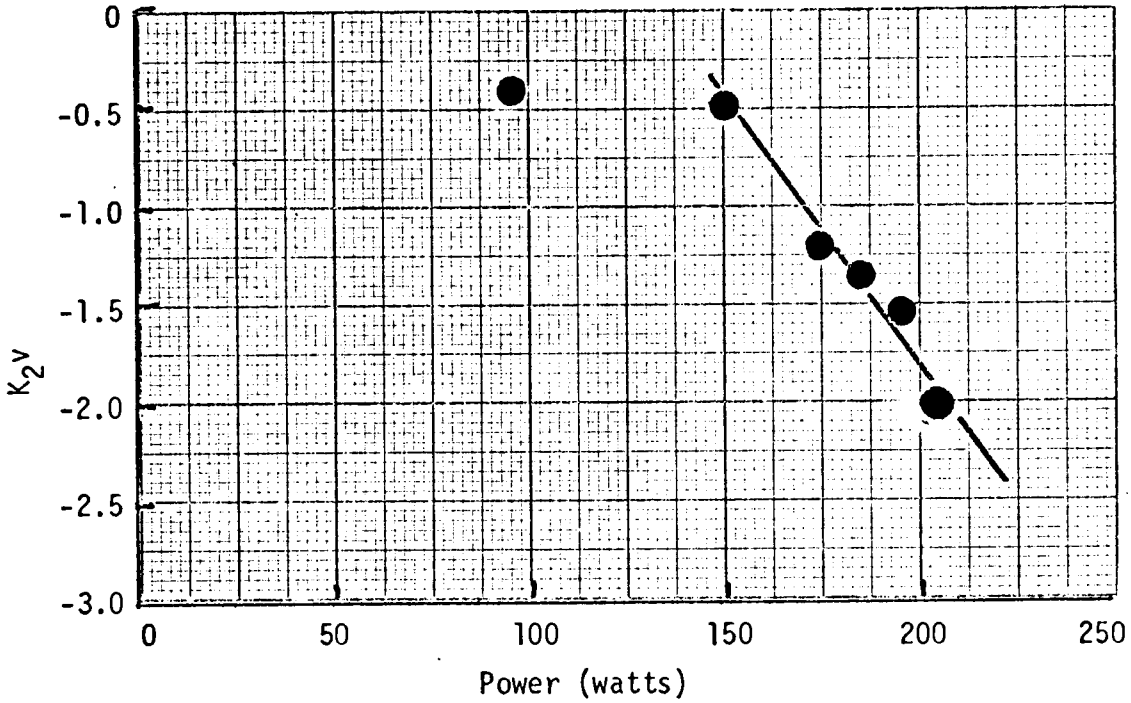

MASSACHUSETTS INSTITUTE OF TECHNOLOGY
SCHOOL OF CHEMICAL ENGINEERING PRACTICE
AT
OAK RIDGE NATIONAL LABORATORY

K_2v as a Function of Power

DATE	DRAWN BY	FILE NO.	FIG.
6-3-69	WAH	CEPS-X-84	6

3. Gas loading increases with increasing power input at a constant liquid flow rate.

4. Gas loading decreases with increasing liquid flow rate at a constant power input.

5. Gas loading is independent of impeller geometry at constant power input to the impeller motor.

6. Over short periods of time the foam exhibits Newtonian characteristics up to a loading of 23%.

7. A flow system is operationally feasible for the production of foams in highly viscous liquids.

7. RECOMMENDATIONS

1. Further work should be done to extend the proposed mixing model along the following lines:

   a. Determine the volumetric gas loading as a function of liquid flow rate and power for fluids of higher viscosities.

   b. Determine the effect of the mixing volume on the percent loading for the present experimental apparatus.

   c. Determine the effect of low liquid flow rates on the percent loading.

2. Temperature and gas loading greatly affect the viscosity of the polybutene, and these variables should be extensively studied in future work.

3. A new impeller bearing should be installed in the impeller motor mount to withstand speeds up to 20,000 rpm.

4. An accurate flow control meter should be installed to regulate the polybutene feed rate.

5. Specific power input data should be obtained for eventual scaleup of the system.

8. ACKNOWLEDGEMENT

The authors would like to express their grateful appreciation for the guidance and assistance given by W.E. Clark, W.F. Schaffer, Jr., and D.E. Spangler.

9. APPENDIX

9.1 Physical Properties of Polybutene 16

Physical properties of the fluid used in this study are summarized in Table 1.

Table 1. Physical Properties of Oronite Polybutene Grade 16 (Produced by the Oronite Div. of Chevron Chemical Co.)

	Manufacturer's Data (11)	Measured
Condition	clear, bright, and free from sediment	
Color	light yellow	light yellow
Specific gravity	0.880 at 60/60°F	0.872 at 80°F
Number average molecular weight	640	-
Viscosity at 80°F	21 poise	22 poise
Temperature Coefficient of Viscosity, $d(\ln\mu)/d(1/T)$	7500	3700
Surface tension	-	31.9 dynes/cm

9.2 Experimental Data

The data used in constructing Figs. 3 and 4 are given in Tables 2 and 3.

Table 2. Variation of Loading as a Function of Impeller Pitch (Power input = 155 w, L = 73 ml/min)

Run No.	Impeller Pitch	$\emptyset$	ω (rpm)	L (ml/min)	Gas Pressure (psig)
1	0°	17.5	3440	73	0.26
2	15°	14.2	-	75	0.28
3	30°	17	3800	73	-
4	45°	15.6	2600	74	0.28
5	90°	13.6	2540	73	0.27

Table 3. Gas Loading Experiments

Run No.	Outlet Temperature (°C)	L (ml/min)	P (watts)	ω (rpm)	Ø (vol %)	Gas Pressure (psig)
A	34	163	155	2350	11.1	1.08
B*	35	188	192	4400	12.8	1.04
C	38	166	189	6900	22.4	1.08
D	35	175	165	3800	14.1	1.04
E	28	650	187	3000	4.1	7.6
F	32	717	221	5000	21.9	7.3
G	29	500	170	2140	1.1	7.3
H	30	540	208	-	20.2	6.7
I	38	95	146	3600	11.3	0.23
J	29	173	96	800	2.1	1.17

Constant impeller pitch = 90°.

*Not used in power curve because of binding of the impeller bearing.

9.3 Viscosity Measurements

The measured viscosities of pure polybutene and of the foams obtained from the experiments presented in Sect. 4.2 are shown in Table 4. The listed foam viscosities were measured at the system temperature and are compared to the viscosity of pure polybutene measured at that temperature. (There was a one to two degree temperature drop while the viscosity measurement was being made.) Viscosities were measured with a Brookfield rotating cylinder viscometer and were calculated using the equation:

$$\mu = \left(\frac{T}{4\pi\ h\omega}\right)\left(\frac{1}{R_b^2} - \frac{1}{R_c^2}\right)$$

where ω is the angular velocity of rotation, T is the torque (equal to full-scale torque times the viscometer scale reading/100), h is the submerged depth of the bob, R_b is the radius of the bob, and R_c is the radius

Table 4. Polybutene Foam Viscosities at Different Volumetric Percent Gas Loadings

Percent Loading	T (°C)	μ_f (poise)	μ_{pb} (poise)	μ_f/μ_{pb}
22.4	36	19	15	1.27
21.9	32	25	17	1.47
20.2	30	25	19	1.32
14.1	35	22	16	1.37
12.9	37	17	15	1.16
12.8	35	23	16	1.44
11.3	38	16	14	1.14
11.1	34	28	16	1.75
9.1	39	16	14	1.14
4.1	28	24	20	1.2
3.1	32	21	17	1.23
2.1	29	22	19	1.16

of the outside cylinder. As a check on the accuracy of measurement, the viscosity of pure polybutene was measured several times at room temperature with the measurements reproducible within 10%.

It was found that up to gas loadings of 22.4%, the maximum obtained in this study, the foams exhibited Newtonian characteristics. Pure polybutene was also Newtonian. As shown in Table 4, the viscosity of the polybutene foam was slightly greater than that for pure polybutene. The scatter is too great to determine a correlation between viscosity and percent loading, although the literature (1, 14) indicates that the viscosity of a foam should increase with loading.

From the discrepancies in the data, it is quite evident that there was considerable error in measuring foam viscosities. The discrepancies probably result from the fact that foam viscosities were measured at temperatures higher than room temperature, which tended to make the foams less stable. Therefore, considerable error was introduced because of the inability to retain a constant elevated temperature and a fixed, homogeneous loading. Determining the degree to which high temperature and the segregation of the foam interacted to affect the viscosity measurements was not possible.

9.4 Location of Original Data

The original data are located on pages 40-49 of Databook A-4477-G. This book together with the calculation file is located at the M.I.T. School of Chemical Engineering Practice, Bldg. 1000, ORNL.

9.5 Nomenclature

h submerged depth of viscometer bob, cm

k_1, k_2 rate constants

L liquid flow rate, ml/min

N number of bubbles

P input power, watts

R_b radius of viscometer bob, cm

R_c radius of cylinder, cm

T torque of viscometer, dyne-cm

v volume of bubbles, cm^3

V volume of foam in mixing chamber, cm^3

$\emptyset$ volumetric gas loading, %

μ viscosity, poise

θ time, sec

τ residence time, sec

ω angular velocity of rotation of viscometer bob, rev/min

9.6 Bibliography

1. Bikerman, J.J., J.M. Perri, R.B. Booth, and C.C. Currie, "Foams: Theory and Industrial Applications," pp. 114-136, Reinhold, New York (1953).

2. "Impeller Type Mixers," A.I.Ch.E. Equipment Testing Procedures, September 1959.

3. Jorris, M.H., and L.S. Bowers, "A Study of the Dispersion of Gases in Viscous Liquids with Application to Radioactive Krypton and Xenon Disposal, Part 1," ORNL-MIT-81, M.I.T. School of Chemical Engineering Practice, ORNL (May 8, 1969).

4. Metzner, A.B. in E.C. Bernhardt (ed.) "Processing of Thermoplastic Materials," Reinhold, New York (1959).

5. Metzner, A.B., and J.C. Reed, "Flow of Non-Newtonian Fluids - Correlation of the Laminar, Transition, and Turbulent-Flow Regions," A.I.Ch.E. Journal, 1, 434 (1955).

6. Metzner, A.B., and R.E. Otto, "Agitation of Non-Newtonian Fluids," A.I.Ch.E. Journal, 3, 3 (1957).

7. Metzner, A.B., in T.B. Drew and J.W. Hoopes, Jr. (eds.), "Advances in Chemical Engineering," Vol. 1, pp. 79-150, Academic Press, New York (1956).

8. "Oronite Polybutenes," Oronite Division of Chevron Chemical Company (1963).

9. Rushton, J.H., E.W. Costich, and H.J. Everett, "Power Characteristics of Mixing Impellers," Chem. Eng. Progr., 46, 395 and 470 (1950).

10. Rushton, J.H., and J.Y. Oldshue, "Mixing - Present Theory and Practice," Chem. Eng. Progr., 49(4), 161 (1953).

11. Sachs, J.P., and J.H. Rushton, "Discharge Flow from Turbine-Type Mixing Impellers," Chem. Eng. Progr., 50, 597 (1954).

12. Shinnar, R., "On the Behavior of Liquid Dispersion in Mixing Vessels," J. Fluid Mech., 10, 259 (1961).

13. Sprow, F.B., "Distribution of Drop Sizes Produced in Turbulent Liquid-Liquid Dispersion," Chem. Eng. Sci., 22, 435 (1967).

14. Vermeulen, T., C.M. Williams, and G.T. Langlois, "Interfacial Area in Liquid-Liquid and Gas-Liquid Agitation," Chem. Eng. Progr., 51, 2 (1955).

INTERNAL DISTRIBUTION

1. E.H. Acree
2. R.E. Blanco
3. J.O. Blomeke
4. R.E. Brooksbank
5. F.M. Browder
6. K.B. Brown
7-12. W.E. Clark
13. W. Davis, Jr.
14. D.E. Ferguson
15. C.L. Fitzgerald
16. A.P. Fraas
17. E.J. Frederick
18. H.W. Godbee
19. H.E. Goeller
20. P.A. Haas
21. Lewis Nelson
22. J.P. Nichols
23. W.F. Schaffer
24. W.E. Unger
25. M.E. Whatley
26. R.G. Wymer
27. Oak Ridge Engineering Practice School
28-29. Central Research Library
30. Document Reference Section
31-33. Laboratory Records
34. Laboratory Records, ORNL R.C.
35. ORNL Patent Office
36-50. M.I.T. Station Files

EXTERNAL DISTRIBUTION

51. W.G. Belter, AEC, Washington
52. Manson Benedict, MIT
53. S.M. Fleming, MIT
54. E.A. Mason, MIT
55. C.W. Selvidge, MIT